

COMPOSITIONAL CLUES TO THE ORIGIN OF REFRACTORY METAL NUGGETS, PEROVSKITE, AND Zr-RICH OXIDES IN HIBONITE FROM THE PARIS CM CHONDRITE. J. Han¹ and L. P. Keller²,
¹Department of Earth and Atmospheric Sciences, University of Houston, Houston TX, 77204, USA (jhan28@central.uh.edu), ²ARES, NASA Johnson Space Center, 2101 NASA Parkway, Houston, TX 77058, USA.

Introduction: Rare Ca-Al-rich inclusions (CAIs) in carbonaceous chondrites are dominated by Zr-, Sc-, Ti-, and/or Y-rich oxides and silicates, and often contain refractory metal nuggets (RMNs) [1-3]. These phases have ultrarefractory (UR) rare earth element (REE) patterns that are complementary to Group II patterns [4]. Therefore, studies of such UR CAIs likely decipher a record of nebular conditions and processes at higher temperatures than other CAIs consisting mainly of spinel and melilite.

Our previous TEM analyses reported a discovery of the assemblages of RMNs, perovskite, and Zr-rich oxides in hibonite from the Paris CM chondrite [5]. Here we present TEM results of a detailed chemical study of these UR phases to provide clues to their formation conditions in the early solar nebula.

Methods: The FIB sections from platy hibonite crystal sample Pmt1-15 were re-examined using a JEOL 2500SE field emission STEM equipped with a JEOL silicon drift detector for energy dispersive X-ray (EDX) analyses at NASA Johnson Space Center. Elemental X-ray maps were obtained using STEM raster mode with a scanned probe size of 1 nm or 2 nm and a dwell time of 50 μ s/pixel. Data reduction was performed using the Cliff-Lorimer thin film approximation with K-factors determined from natural and synthetic standards. However, calculated K-factors for Sc, Zr, Y, and refractory metals were used to estimate their concentrations in EDX spectra.

Results & Discussion:

1. Perovskite and Zr-rich oxides. In Pmt1-15, there are three texturally and compositionally different occurrences of perovskite (**Fig. 1**; average wt% are provided here): (1) micrometer-sized perovskite grains are attached to lakargiite or tazheranite and contain 2.9 wt% Al_2O_3 , 4.7 wt% Y_2O_3 , and 8.1 wt% ZrO_2 ; (2) perovskite laths are crystallographically oriented to hibonite and contain 2.7 wt% Al_2O_3 , 1.7 wt% Y_2O_3 , and 1.8 wt% ZrO_2 ; and (3) rounded perovskite nanoparticles at the hibonite-hibonite grain boundaries contain 2.4 wt% Al_2O_3 and 2.1 wt% Y_2O_3 .

Lakargiite, $(\text{Ca}_{0.97}\text{Y}_{0.03})(\text{Zr}_{0.61}\text{Ti}_{0.35}\text{Al}_{0.04})\text{O}_3$, contains ~ 1 wt% Al_2O_3 and 2.3 wt% Y_2O_3 . Tazheranite, $(\text{Zr}_{0.56}\text{Ca}_{0.19}\text{Y}_{0.08}\text{Sc}_{0.08}\text{Ti}_{0.08}\text{Al}_{0.02})\text{O}_{1.74}$, is Sc-Y-rich, with 4.4-6.1 wt% Sc_2O_3 and 8-9.8 wt% Y_2O_3 .

The increased Al_2O_3 , Y_2O_3 , and ZrO_2 concentrations in perovskites in Pmt1-15, together with the occurrence of lakargiite and tazheranite, suggest that they formed from very high-temperature processes that allowed the

incorporation of more refractory Al, Y, and Zr into perovskite and expanded the stability field of Zr-rich oxides relative to Ca-Al-oxides (i.e., corundum). However, the observed variations in Al, Y, and Zr abundances in three perovskite types and their textural and mineralogical differences suggest distinct formation conditions. Y-Zr-rich perovskite may have formed probably after lakargiite and tazheranite, at higher temperatures than perovskite laths and nanoparticles that contain lower concentrations of Y_2O_3 and ZrO_2 .

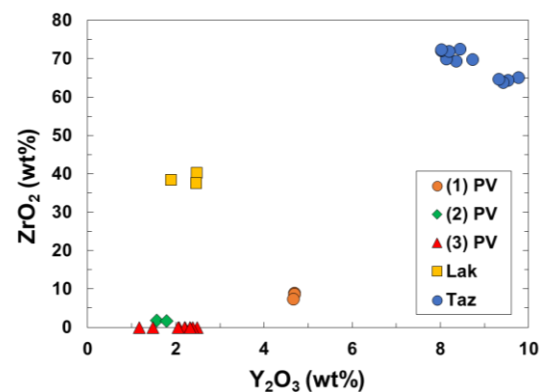


Figure 1. A plot of ZrO_2 vs. Y_2O_3 in different perovskite types, lakargiite, and tazheranite from Paris hibonite Pmt1-15.

2. Refractory Metal Nuggets. A total of 82 RMNs were identified in hibonite, perovskite, lakargiite, and tazheranite from Pmt1-15. They range from 10-350 nm in size and display a variety of morphologies from anhedral to fully euhedral, but most have straight faces in our FIB cross sections [5]. RMNs are often associated with nanometer-sized perovskite and Zr-rich oxide.

Thirty-four RMNs were analyzed by EDX to determine their composition. All RMNs are chemically homogenous crystals, with no evidence for zonation within the grains. Refractory siderophile elements and Fe were detected in varying abundances among the nuggets, but Pt and Ni were below detection limits. No correlation between the RMNs' composition and their host phases was observed.

Based on the Os contents of RMNs, we identify two compositional groups. (1) Twenty-nine RMNs are strongly enriched in Re (4.0-7.7 wt%), Os (64.9-78.1 wt%), and W (9.2-12.6 wt%), and contain Ir, Mo, Ru, and Fe. These nuggets all occur in hibonite, perovskite, lakargiite, and tazheranite. The RMNs have Re/W ratios of 0.4-0.69 scattered around or above a solar value ($=0.42$; [6]), but their Ir/Os ratios of 0.06-0.19 are much

lower than a solar value ($=0.95$; [6]). In addition, the CI-normalized abundance pattern of these nuggets shows similar enrichments ($\sim 10^6 \times \text{CI}$) of Re, Os, and W and decreasing enrichments from Ir to Fe, often with a Mo depletion relative to Ru (**Fig. 2a**).

(2) Four RMNs are enriched in Os (27.8-46.5 wt%) and Ir (26-33 wt%), and contain Re, W, Mo, Ru, and Fe. They occur in hibonite or along the hibonite-tazheranite grain boundary, but near Group 1 nuggets. These nuggets have Re/W ratios of 0.24-0.45 close to or below the solar value, and their Ir/Os ratios show a wider range of 0.56-1.1. The CI-normalized abundance pattern of three RMNs have similar enrichments ($\sim 6-7 \times 10^5 \times \text{CI}$) of Re, Os, W, and Ir, with a Mo depletion relative to Ru. In contrast, one nugget contains a lower Re abundance ($\sim 2 \times 10^5 \times \text{CI}$), with a relative depletion of W and Mo, with the Mo depletion being larger, but at the similar degree to other three (**Fig. 2b**).

The elemental abundances and patterns determined from RMNs in Pmt1-15 provide unique insights on their formation conditions in the early solar nebula. Group 1 RMNs have much higher Re and Os contents, compared to any RMNs reported previously from carbonaceous chondrites (≤ 4 wt% Re and 1.5-47 wt% Os; [7-9]). Because Re and Os condense first [6], these Re-Os-W-rich RMNs represent the highest temperature nebular products that likely served as the nucleation sites for other UR phases. In addition, the occurrence of Group 1 RMNs all in hibonite, perovskite, lakargiite, and tazheranite suggests their formation before any of these refractory oxides. The elemental ratios of Group 1 RMNs match closely with those predicted to condense at $\sim 1650\text{K}$ at 10^{-4} bar [9-10], higher than temperatures at which hibonite and perovskite begin to condense, i.e., 1647K and 1609K at 10^{-4} bar [11].

In comparison with Group 1, Group 2 RMNs show more flattened patterns with increased enrichments in Ir, Mo, and Ru. This compositional difference indicates their formation at slightly lower temperatures than Group 1 RMNs from a partially-condensed gas

containing some fractions of Re, Os, and W. A comparison of elemental ratios measured from Group 2 RMNs with those calculated for equilibrium condensation models also suggests their formation at $<1500\text{K}$ at 10^{-4} bar [9-10]. However, the proximity between Group 1 and 2 RMNs in hibonite suggests that their formation temperature gap was not as large as estimated from equilibrium condensation models.

We hypothesize a fractional condensation scenario: the ultra-refractory Re-Os-W-rich alloy (Group 1) condensed first from a gas at higher temperatures than any of CAI oxides. The less-refractory Ir-Mo-Ru-rich alloy (Group 2) eventually condensed from the residual metals in the gas, probably before hibonite and after perovskite and Zr-rich oxides. The small Mo depletion in elemental abundance patterns of many RMNs suggests their formation under slightly oxidizing conditions [12].

An unusual RMN #A-11 in tazheranite appears an aggregate of two crystals that are compositionally complementary to each other, with one enriched in Os, Ir, and Ru and the other enriched in W and Mo (**Fig. 2c**). This compositional difference may be a result of the segregation of bcc W and Mo from hcp Os and Ru, while fcc Ir was preferentially incorporated into the hexagonally close-packed (001) faces [7]. In contrast, all other RMNs are compositionally homogenous, single crystals. Further TEM study is underway to test if they nucleated and grew as hcp structured crystals [7].

References: [1] Krot A. N. et al. (2019) *Geochemistry* 79, 1255-19. [2] Ma C. et al. (2020) *GCA* 277, 52-86. [3] Xiong Y. et al. (2020) *MAPS* 55, 2184-2205 [4] Genzel P. T. et al. (2020) LPSC, abstract #2002. [5] Han J. et al. (2021) LPSC, abstract #2587. [6] Palme H. et al. (2014) In: *Treatise on Geochemistry*, pp.15-36. [7] Harries D. et al. (2012) *MAPS* 47, 2148-2159. [8] Schwander D. et al. (2014) *MAPS* 49, 1888-1901. [9] Schwander D. et al. (2015) *GCA* 168, 70-87. [10] Berg T. et al. (2009) *Astro J* 702, L172-L176. [11] Yoneda S. and Grossman L. (1995) *GCA* 59, 3413-3444. [12] Fegley B. Jr. and Palme H. (1985) *EPSL* 72, 311-326.

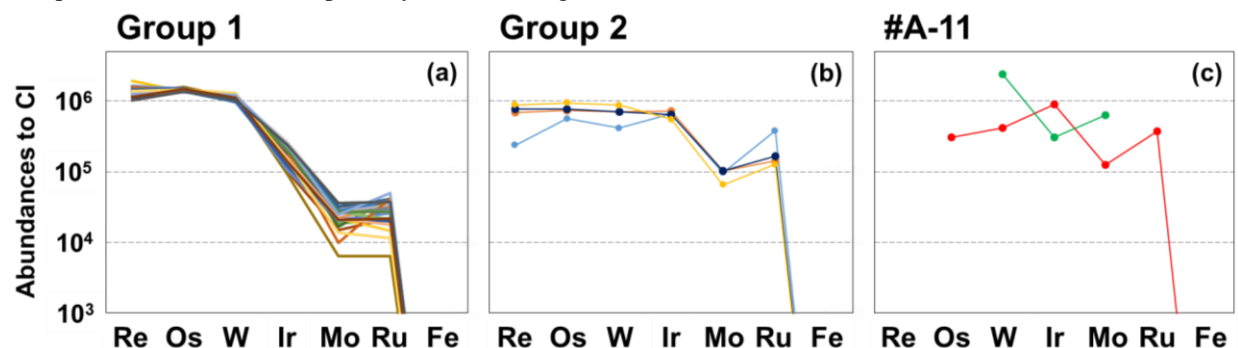


Figure 2. Elemental abundances relative to CI chondrites [6] of RMNs from Paris hibonite Pmt1-15. Refractory siderophile elements on the x axis are plotted in order of increasing volatility. The Fe contents in all RMNs are very low, with up to 1.2 wt%.